Article

# 3D DNA Nanomachine Biosensor by Integrating DNA Walker and Rolling Machine Cascade Amplification for Ultrasensitive Detection of Cancer-Related Gene

Na Wu, Kun Wang, Yi-Ting Wang, Ming-Li Chen, Xuwei Chen, Ting Yang, and Jian-Hua Wang

*Anal. Chem.*, **Just Accepted Manuscript** • DOI: 10.1021/acs.analchem.0c01074 • Publication Date (Web): 09 Jul 2020

# 3D DNA Nanomachine Biosensor by Integrating DNA Walker and Rolling Machine Cascade Amplification for Ultrasensitive Detection of Cancer-Related Gene

*Na Wu†, Kun Wang†, Yi-Ting Wang, Ming-Li Chen, Xu- Wei Chen, Ting Yang*, Jian-Hua Wang*

*Research Center for Analytical Sciences, Department of Chemistry, College of Sciences, Northeastern University, Box 332, Shenyang 110819, China*

*E-mail: yangting@mail.neu.edu.cn (T. Yang).

**ABSTRACT**

Stochastic DNA walkers capable of traversing on three-dimensional (3D) tracks have received great attentions. However, DNA walker-based biosensors exhibit limited amplification efficiency due to their slow walking kinetics and low processivity. Herein, by taking advantage of the high processivity of DNA rolling machine, a sensitive ratiometric DNA nanomachine biosensor is designed. The biosensor is constructed with hairpin-loaded AuNPs (hpDNA@AuNPs) as DNA walker and AgNCs-decorated magnetic NPs (AgNCs@MNPs) as DNA rolling machine. In the presence of target DNA, exonuclease III (Exo III)-powered DNA walker is activated to accomplish first stage amplification via a burnt-bridge mechanism, generating a great deal of toehold-loaded AuNPs (Toehold@AuNPs) to hybridize with AgNCs@MNPs with the assistance of Exo III. These triggers rapid rolling of AuNPs on AgNCs@MNPs surface and releases free AgNCs, converting the biological signal into mass spectrometric signal ratio ($^{107}$Ag /$^{197}$Au) with detection by ICP-MS. A linear range of 0.5-500 fmol $L^{-1}$ is achieved with a detection limit of 119 amol $L^{-1}$ for p53 gene. The practical applicability of the biosensor has been demonstrated in the accurate assay of p53 gene in human blood.

**KEYWORDS:**

DNA walker; DNA rolling machine; Exo III; cascade amplification; ICP-MS

## INTRODUCTION

DNA walking machines are a new class of molecular machine that move along prescribed one-, two- or three-dimensional DNA tracks.[1, 2] DNA walking machines have found wide application in biosensing, cargo delivery and biocomputing due to their remarkable mechanical motion, high directionality and exquisite programmability.[3] In particular, three-dimensional (3D) DNA walkers that constructed on the surface of micro- or nanoparticles have drawn extensive interest in biosensing applications.[4-12] Compared with their one-dimensional (1D) and two-dimensional (2D) counterparts, 3D DNA walkers possess high DNA loading capability, thus strikingly enhances the local concentration of track DNA for improved walking efficiency and higher processivity.[1] In the analytical point of view, rapid walking kinetics and high processivity facilitate high signal gain in a given time.[13] Therefore, 3D DNA walker is regarded as ideal tools for signal transduction and amplification. However, most of 3D DNA walkers move in a "step-by-step" way, during which process the walking leg is prone to derail the track.[13, 14] Once the walking leg is detached from the DNA track, the walking terminates and the signal amplification stops,[14-18] this makes 3D DNA walker-based sensors not as sensitive as they are expected.

Recently, a high-speed DNA rolling machine that moves along RNA tracks propelled by RNase H was reported.[19] By changing the moving mode from walking to rolling, the processivity was strikingly improved by three orders of magnitude, as the derailment of leg DNA was largely reduced. This kind of biosensors would be faster and more sensitive, as demonstrated by an electrochemiluminescence biosensor based on a $Zn^{2+}$-driven DNA rolling machine.[13] As far as we know, most DNA rolling machines reported hitherto rolls on a 2D DNA track, i.e., they are essentially 2D DNA

rolling machines.[13, 14, 19] Herein, for the first time, we construct a 3D DNA rolling machine, with DNA-conjugated AuNPs rolling along the surface of DNA-loaded magnetic nanoparticles. It inherits the advantage of 3D DNA walkers of high DNA enrichment capability and high signal amplification ability. With p53 as a model target, a novel biosensor is designed for ultrasensitive ratiometric detection of biomarker based on a cascade amplification strategy, i.e., 3D DNA walker coupled with 3D DNA rolling machine.

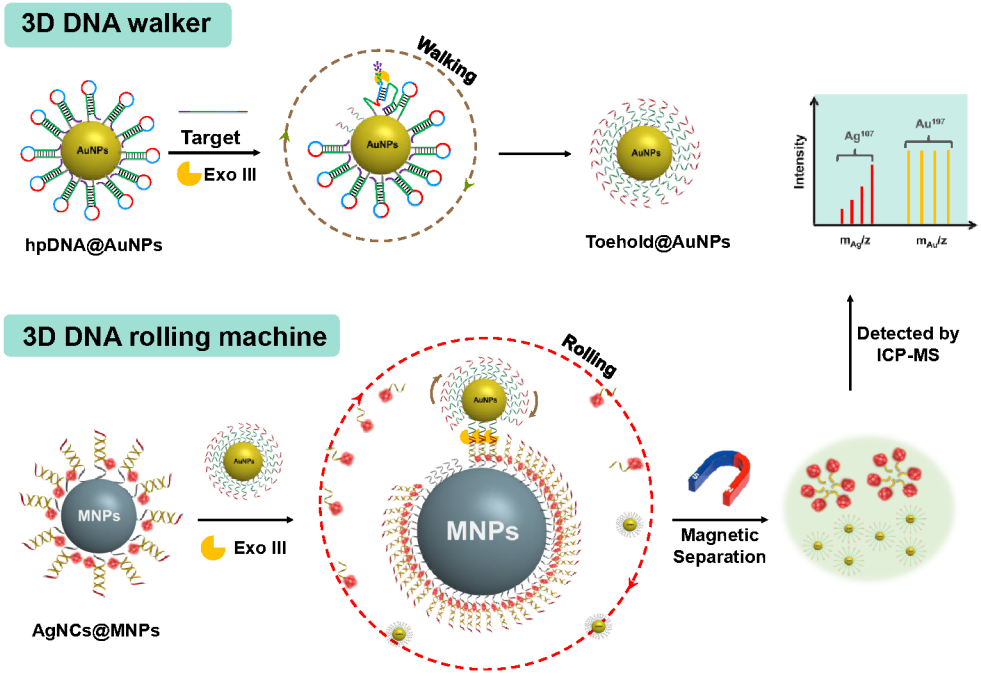


Scheme 1. Schematic illustration of the cascade amplification strategy of 3D DNA walker coupled with 3D DNA rolling machine. hpDNA@AuNPs: hairpin DNA conjugated AuNPs; Toehold@AuNPs: toehold DNA conjugated AuNPs; AgNCs@MNPs: DNA@AgNCs conjugated magnetic nanoparticles; Exo III: exonuclease III. In the first stage, target DNA walks along the surface of hpDNA@AuNPs, and trims hpDNA into toehold DNA; in the second stage, Toehold@AuNPs roll on the surface of AgNCs@MNPs, releasing AgNCs into the supernatant; after magnetic separation, the mass spectrometric signal ratio ($^{107}$Ag /$^{197}$Au) is measured by ICP-MS as signal output.

As illustrated in Scheme 1, hairpin DNA conjugated-AuNPs (hpDNA@AuNPs) are employed as 3D DNA walker with target DNA (p53) acting as walkable leg, and magnetic nanoparticles loaded with AgNCs-labeled DNA (AgNCs@MNPs) are employed as the 3D DNA rolling machine for AuNPs to roll on. Both the DNA walker and rolling machines are fueled by exonuclease III (Exo III). In the first stage

amplification, the hairpin DNA on AuNPs surface is first opened up by hybridizing with target DNA (p53) to form blunt-end dsDNAs, which act as fuel DNA and are cleaved by Exo III. As Exo III digests hpDNA strand from the 3' end, target DNA is partially free and hybridizes with adjacent hpDNA simultaneously. This facilitates target DNA to walk along the surface of hpDNA@AuNPs and trims hpDNA into residue ssDNA (toehold DNA) at the same time. In the second stage amplification, toehold DNA partially hybridizes with AS DNA on magnetic nanoparticles (MNPs) surface and initiates the Exo III digestion of AS DNA. As dozens of DNAs are cleaved by Exo III at the same time, Toehold@AuNPs roll on the surface of MNPs and release the pre-hybridized AgNCs, facilitating the second stage amplification. In this way, a few inputs of target DNA may result in great signal gain with detection by either fluorescence or ICP-MS. Gold nanoparticles (AuNPs) are used not only as carrier motor but also as internal standard in ICP-MS detection. In addition, the two stages of amplification employ a same enzyme (Exo III), the step-by-step amplification is integrated into one-step, which largely simplifies the sensing process.

## EXPERIMENTAL SECTION

**Preparation of gold nanoparticles.** The citrate-stabilized gold nanoparticles (AuNPs) with 10 nm diameter were prepared as previously reported.[20] In brief, 10 mL of $HAuCl_4$ (1 mmol $L^{-1}$) solution was heated to boiling temperature with stirring. Then, 1 mL of sodium citrate (40 mmol $L^{-1}$) was added to the boiling solution. It was heated for another 10 min until the final color changes to wine red. After cooling down to room temperature, AuNPs were stored at 4 °C for further use.

**Preparation of hairpin DNA (hpDNA) conjugated AuNPs (hpDNA@AuNPs).** First, 100 μL of thiolated hpDNA (6 μM) was incubated with 20

μL of TCEP (50 mmol $L^{-1}$, pH 7.4) for 1 h to avoid disulfide formation. Then, 140 μL of PB buffer solution (1.9 mmol $L^{-1}$ $NaH_2PO_4$ and 8.1 mmol $L^{-1}$ $Na_2HPO_4$, pH 7.4) and 500 μL of AuNPs (1.69 nM) were added into 120 μL of the above solution. The mixture was allowed to react for 5 h at 35 °C. Afterwards, 30 μL of aging buffer solution (10 mmol $L^{-1}$ PBS, 2 M NaCl, 1 mmol $L^{-1}$ EDTA) was added into the above reaction mixture every 30 min until the final concentration of NaCl reached 0.6 mmol $L^{-1}$. The salting process was followed by overnight-incubation at 35 °C. Finally, the excessive hpDNA was removed by centrifugation twice at 14000 rpm for 15 min. The hpDNA conjugated AuNPs (hpDNA@AuNPs) were finally resuspended in 1 mL of 10 mmol $L^{-1}$ PBS buffer and stored at 4 °C for further use.

**Synthesis of DNA@AgNCs.** AgNCs were prepared as previously reported.[21] Briefly, 100 μL of $DNA_{Ag}$ solution (10 μmol $L^{-1}$) was mixed with 20 μL of $AgNO_3$ (600 μmol $L^{-1}$) and incubated in ice water for 30 min. Then, 20 μL of freshly-prepared $NaBH_4$ (600 μmol $L^{-1}$) was added into the above mixture with vigorous shaking for 1 min and then incubated in dark for 5 h before use.

**Preparation of AgNCs-conjugated MNPs (AgNCs@MNPs).** $NH_2$-terminated anchor strand (AS) was coupled to carboxyl magnetic nanoparticles (MNPs) by a single-step carbodiimide reaction. Briefly, 1 mL of MNPs (5 mg $mL^{-1}$) was washed with 1 mL of MES buffer (100 mmol $L^{-1}$, pH 5.0) for three times and resuspended in 1 mL of the same buffer. Afterwards, MNPs were activated by reacting with 200 μL of EDC (1 mg $mL^{-1}$) and 200 μL of NHS (1 mg $mL^{-1}$) for 60 min at room temperature. Then, the activated MNPs were washed for three times with MES buffer and resuspended in 1 mL of TE-$Mg^{2+}$ buffer (10 mmol $L^{-1}$ Tris, 10 mmol $L^{-1}$ $MgCl_2$, 0.1% tween-20 pH 7.4). 100 μL of $NH_2$-teminated AS (6 μmol $L^{-1}$) were added into the activated MNPs solution and incubated overnight at 25 °C. After incubation, the

AS-conjugated MNPs (AS@MNPs) were washed with TE-$Mg^{2+}$ buffer for three times and suspended in Tris-HCl buffer (10 mmol $L^{-1}$ Tris, 4 mmol $L^{-1}$ $MgCl_2$, 0.05% BSA, 0.1% tween-20, pH 7.4) for 60 min to block the non-specific binding sites. Thereafter, the AS@MNPs were washed with TE-$Mg^{2+}$ buffer for three times and resuspended in 1 mL of TE-$Mg^{2+}$ buffer. In the following, 100 μL of DNA@AgNCs were added to hybridize with AS@MNPs at 35 °C for 12 h. Finally, the excessive DNA@AgNCs were removed by magnetic separation. The resulting AgNCs@MNPs were washed with 200 μL of TE-$Mg^{2+}$ buffer (pH 7.4) for three times and resuspended in 500 μL of the same buffer and stored at 4 °C for further use. The prepared AgNCs@MNPs were characterized by confocal fluorescence microscope and fluorescence spectrophotometer with both excitation and emission slits of 10 nm and voltage of 700 V. The fluorescence was detected at $\lambda_{ex}/\lambda_{em}$ 528/641 nm.

**Exo III-Assisted target cascade amplification**. 20 μL of hpDNA@AuNPs, 40 μL of AgNCs@MNPs, 10 μL of Exo III (10 U/100 μL) and 10 μL of reaction buffer (50 mmol $L^{-1}$ Tris-HCl, 5 mmol $L^{-1}$ $MgCl_2$, 1 mmol $L^{-1}$ DTT) were mixed with 20 μL p53 of various concentrations. The mixture was incubated at 35 °C with gentle shaking at 156 rpm for 50 min. Thereafter, the above mixture was heated at 70 °C for 20 min to stop the enzyme reaction. After magnetic separation, the supernatant was digested with aqua regia followed by appropriate dilution for ICP-MS measurement (Caution: aqua regia is a powerful oxidizing reagent, and it should be handled with extreme care).

**Gel electrophoresis analysis.** Non-denaturating polyacrylamide gel electrophoresis (PAGE) was used to further confirm the reaction products. The concentration of each standard DNA sample was set as 1 μmol $L^{-1}$. A mixture of each sample (10 μL) and loading buffer (2 μL) was added into 15% polyacrylamide gel.

All the prepared gels were run at a constant voltage of 150 V for 45 min in 1× TBE buffer followed by staining with 4S Red Plus for 30 min. Gel images were obtained by an UV digital imaging system (Shanghai Furi Science & Technology Co. Ltd.)

## RESULTS AND DISCUSSION

**Principle of DNA walker cascade amplification strategy.** Scheme 2 depicts the two stages of amplification, i.e., (1) target DNA walking on AuNPs to trim the hairpin DNA into toehold DNA, and (2) AuNPs rolling on MNPs' surface to release AgNCs as signal output, both are fueled by Exo III. In the first stage amplification, AuNPs are conjugated with hundreds of hairpin DNA (hpDNA) strands to serve as 3D DNA track. hpDNA is designed to have an overhang at its 3'-terminus to avoid Exo III digestion and is partially complementary to the target for selective response. As a proof of principle, p53 was chosen as the target DNA. The target DNA hybridizes with hpDNA and forms a blunt end, which is then recognized and digested by Exo III from the blunt 3'-termini. As the digestion of hpDNA proceeds, target DNA is partially released and hybridizes with another hpDNA nearby. In this way, the target walks along AuNPs surface, and hpDNA is trimmed into toehold DNA at the same time (Scheme 2A). In the second stage (Scheme 2B), MNPs are conjugated with anchor strand (AS) for the hybridization with AgNCs-labeled DNA and serve as 3D DNA track for AuNPs to roll on. The overhangs at 3'-termini of both strands protect them from Exo III digestion. The hybridization of toehold DNA and AS DNA generates recessed 3'-terminus, which is soon recognized and digested by Exo III. As there are dozens of toehold DNA strands on AuNPs surface acting as walkable legs, AuNPs roll instead of walking on MNPs surface. The rapid rolling process releases large amount of AgNCs, which may be subsequently quantified by either fluorescence

or ICP-MS.

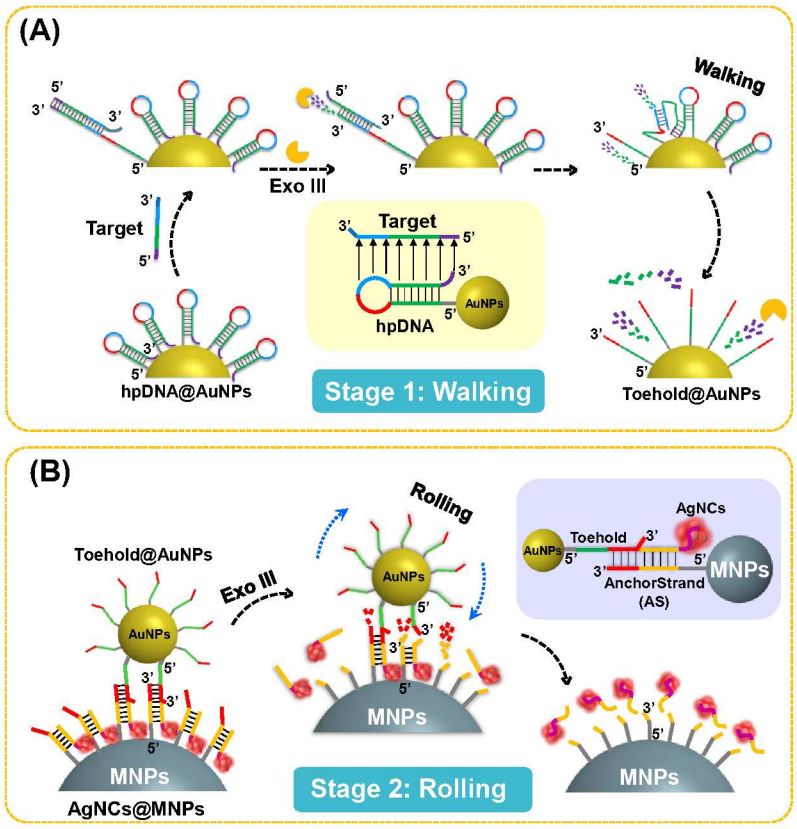


Scheme 2. Schematic illustration of the working principles of (A) walking and (B) rolling. hpDNA@AuNPs: hairpin DNA conjugated AuNPs; Toehold@AuNPs: toehold DNA conjugated AuNPs; AgNCs@MNPs: DNA@AgNCs conjugated magnetic nanoparticles; Exo III: exonuclease III. The sequence of the related DNA strands are shown in Table S1

**Characterizations.** The thio-labeled hpDNA probes were conjugated to AuNPs through Au-S bond with a salt aging method.[22] AuNPs remain wine red after DNA conjugation (Figure S1), indicating no aggregation during the modification process. Meanwhile, a slight red shift in UV-vis absorption spectrum confirmed the formation of hpDNA@AuNPs (Figure S1). In order to calculate the number of DNA strands loaded on each AuNP, FAM-labeled hpDNA was conjugated to AuNPs with the same procedure, and DNA concentration was quantified based on fluorescence intensity of FAM (Details are described in Supporting Information). For 10-nm AuNPs, the average number of hpDNA loaded on each AuNP is derived to be 142 copies at the given experimental conditions. The DNA rolling system was constructed by

functionalizing carboxyl magnetic nanoparticles (MNPs) with $NH_2$-terminated anchor strand (AS) via a single-step carbodiimide reaction, followed by decoration of DNA-templated AgNCs via hybridization. Confocal fluorescent microscope images were used to confirm the decoration of AgNCs on MNPs. As shown in Figure S2A-B, a bright fluorescence is clearly observed for the case of AgNCs@MNPs, whereas virtually no fluorescence is seen on MNPs surface, indicating the formation of AgNCs@MNPs.

**Feasibility of cascade amplification strategy.** The polyacrylamide gel electrophoresis (PAGE) analysis was employed to verify the feasibility of the cascade amplification strategy and the results are shown in Figure 1A. In lane 5, the appearance of a new upper band compared with lane 1 (p53) and lane 2 (hpDNA) demonstrates the efficient hybridization between hpDNA and p53. Similarly, the hybridization between AS and $DNA_{Ag}$ is also confirmed by comparing the bands of lane 3 (AS) and lane 4 ($DNA_{Ag}$) with lane 7 (AS + $DNA_{Ag}$). The hybridization product of hpDNA/p53 can be efficiently digested by Exo III, which is obviously demonstrated by the absence of the hybridization band in lane 6. However, the hybridization product of AS/ $DNA_{Ag}$ is not digested by Exo III, as clearly indicated in lane 7 and lane 8, wherein the intensity of the bands are almost identical regardless the presence of Exo III. It is shown in lane 9 that the mixture of hpDNA, p53, AS and $DNA_{Ag}$ results in the band of hybridization product of hpDNA/p53 and AS/$DNA_{Ag}$ (marked as **), together with a new upper band of the hybridization product of hpDNA/p53/AS/$DNA_{Ag}$ (marked as *). As the probability for the four strands to hybridize into one complex is low, the new upper band is not as bright as that of the two-strand-hybridization band. When Exo III is added into the mixture of the four strands (lane 10), the hybridization bands disappear while a new band with a smaller

molecular weight than that of the two-strand-hybridization band appears. This is ascribed to the intermediate digestion fragment of the hpDNA/p53 (or AS/$DNA_{Ag}$) complex. Afterwards, we allowed AgNCs@MNPs to react with hpDNA@AuNPs, p53 and Exo III for 10 min, 30 min and 50 min, respectively, and the digestion was then terminated. MNPs were magnetically separated and washed for further conducting SEM and TEM imaging analysis. As shown in Figure S3, as the reaction proceeds, more and more AuNPs finish rolling and detach from MNPs surface. Meanwhile, AgNCs are also released into the supernatant, as can be demonstrated by the reduced fluorescence of AgNCs@MNPs after reacting with hpDNA@AuNPs, p53 and Exo III for 30 min (Confocal fluorescent microscope images, Figure S2B-C). Further evidence for the feasibility of the cascade amplification system is shown by ICP-MS analysis. Figure 1B illustrated that only when all the above elements of the biosensing system present, the release of AgNCs is observed along with a 9.2-fold improvement on the signal with respect to that of the background without p53 gene (column 5). This clearly demonstrated that the cascade amplification strategy produces much higher sensitivity for the detection of target DNA.

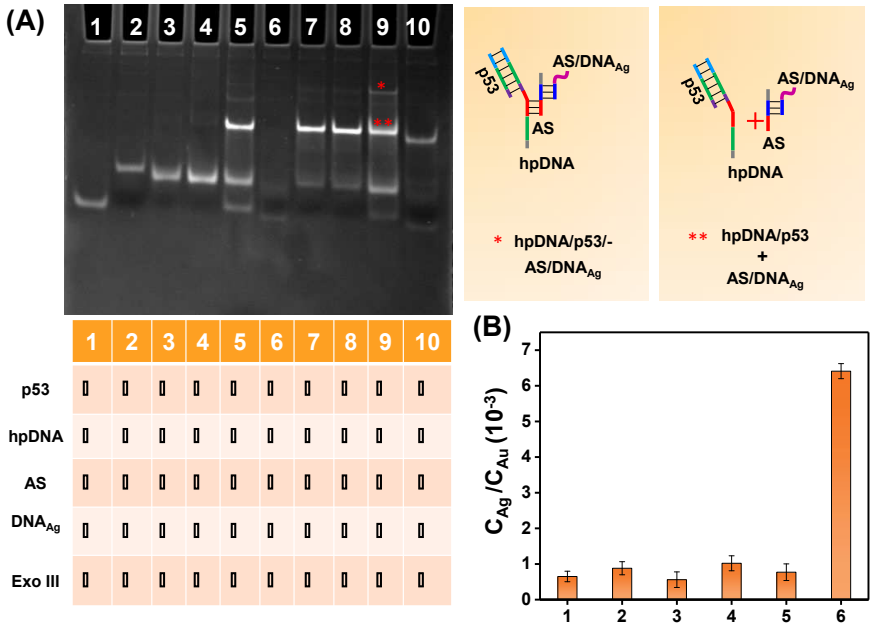

Figure 1. Characterization of cascade amplification of the 3D DNA walker and rolling machine system. (A) PAGE (15% native gel) images. All reactions are run at 25°C for 45 min. The concentration of each standard DNA sample was set as 1 μmol $L^{-1}$. Lanes: (1) p53, (2) hpDNA, (3) AS, (4) $DNA_{Ag}$, (5) mixture of hpDNA and p53, (6) mixture of hpDNA, p53 and Exo III, (7) mixture of AS and $DNA_{Ag}$, (8) mixture of AS, $DNA_{Ag}$ and Exo III, (9) mixture of hpDNA, p53, AS and $DNA_{Ag}$, and (10) mixture of hpDNA, p53, AS, $DNA_{Ag}$ and Exo III. (B) ICP-MS signals of this system at different experimental conditions: (1) hpDNA@AuNPs+p53, (2) hpDNA@AuNPs+p53+Exo III, (3) AgNCs@MNPs+Exo III, (4) AgNCs@MNPs+hpDNA@AuNPs+p53, (5) AgNCs@MNPs+hpDNA@AuNPs+Exo III, (6) AgNCs@MNPs+hpDNA@AuNPs +p53+Exo III. The concentration of p53 is 500 fM.

**Comparison of DNA walking machine with DNA rolling machine.** In order to confirm the improved walking efficiency and signal amplification capability of DNA rolling machine, the kinetics of rolling in the second stage were compared with conventional 3D DNA walker. For the kinetics evaluation of rolling, thiolated toehold DNA was first conjugated with AuNPs using the same experimental conditions as that for the conjugation of hpDNA. The Toehold@AuNPs were then added in AgNCs@MNPs solutions together with Exo III. The mass spectrometric signal of $^{107}Ag$ of the supernatant by ICP-MS was recorded at different time intervals. As for walking mode, all experimental conditions were the same, except that same amount of free toehold strand was used instead of Toehold@AuNPs. As shown in Figure 2, the rolling mode generates faster and higher signal than that of walking mode, confirming that the rolling mode is faster and more efficient than walking.

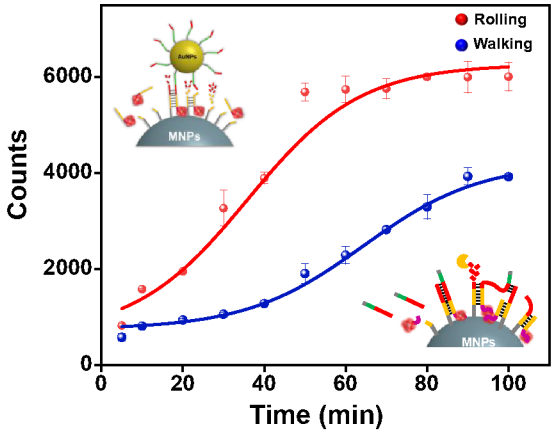


Figure 2. Kinetics comparison between rolling (red circle) and walking (blue circle). All experimental conditions were set the same for rolling and walking: AgNCs@MNPs (40 μL), Exo

III (10 U/100 μL, 10μL) and p53 (500 fM, 20μL). The concentration of free toehold and toehold conjugated with AuNPs was adjusted to the same level using procedure described in SI 1.3.

**The scrutiny of experimental parameters.** Some of the key experimental parameters were thoroughly investigated for optimizing the performance of the biosensing system. These include the density of hpDNA on AuNPs, the length of AS, the dosage of Exo III, the concentration of AS and DNA@AgNCs used for MNPs conjugation, the reaction time, pH and temperature. It is shown in Figure 3A that with the increase of hpDNA density on AuNPs, ICP-MS signal encounters increase followed by decline as the concentration ratio of hpDNA/AuNPs exceeds 360:1. Higher density of hpDNA leads to larger amount of walkable leg for AuNPs, thus accelerates the rolling of AuNPs and improves the signal intensity. However, when the density of hpDNA exceeds a threshold, it will be harder for Exo III to access due to its macromolecular feature (31 KDa), leading to the reduction of signal amplification efficiency.

Exo III-digestion efficiency might be related with the length of the anchor strand (AS), thus we further designed three anchor strands with different lengths and their performances are compared. As is shown in Figure 3B, the biosensor constructed with AS of medium length (29 nt) gives rise to best performance. With a shorter AS (23 nt), the distance between AuNPs and MNPs are smaller, leaving limited room for Exo III to access. On the other, however, if the strands are too long, they tend to lie down on MNPs surface, preventing them from further hybridization.

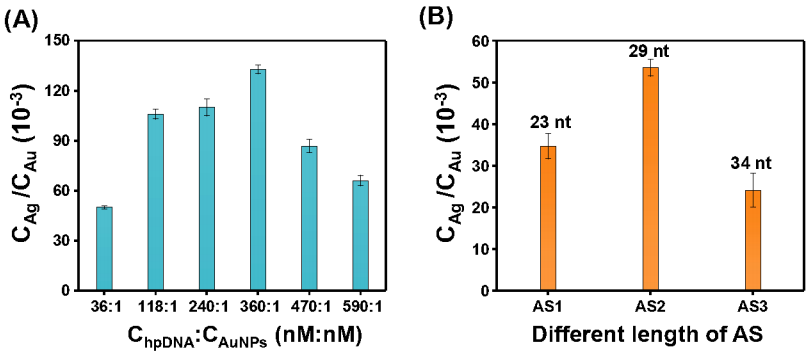

Figure 3. The effect of (A) reaction ratio of hpDNA/AuNPs and (B) the length of AS on the performance of the biosensor. Experimental conditions are the same as described in Experimental sections except the concentration of p53 was set as 1 pM.

Considering that both walking and rolling are fueled by Exo III, the two processes proceeded simultaneously in this study. The time-dependency of the one-step cascade amplification detection was evaluated with the result shown in Figure S4A. It turns out that 50 min suffices the completion of both the walking and rolling process.

The coverage of AS and DNA@AgNCs on MNPs surface would affect the performance of rolling, thus their concentration were also optimized. As is shown in Figure S4B-C, 6 μmol $L^{-1}$ of $NH_2$-teminated AS and 1 μmol $L^{-1}$ of DNA@AgNCs were enough to fully cover the surface of MNPs. Further experiments reveal that larger Exo III dosage helps to improve the signal amplification efficiency, and Exo III functions best at pH 7.5 and 35℃ (Figure S5). As a summary, the construction of the biosensor is conducted by functionalizing AuNPs with hpDNA at a reaction ratio of 360:1, together with MNPs conjugated by AS (29 nt, 6 μmol $L^{-1}$) and DNA@AgNCs (1 μmol $L^{-1}$); the cascade amplification of walking and rolling are proceeded simultaneously at pH 7.5 in a Tris-$Mg^{2+}$ buffer at 35℃, with Exo III concentration of 10 U/100 μL for 50 min.

**Contribution of signal amplification by each stage.** We further compared the signal amplification contribution of each stage by evaluating the improvement of detection limit after each amplification process with p53 as target DNA. For the case without amplification, FAM-labeled hpDNA was conjugated with AuNPs under the same experimental conditions as that for the cascade amplification system in this study. In the absence of target DNA, the fluorescence of FAM was quenched by AuNPs. Once the target DNA was added, the hairpin was opened up and the fluorescence was recovered. By using the fluorescent intensity of FAM for quantification, a detection limit of 280 fM for p53 was obtained (Figure 4A).

By adding Exo III into the above system, the reaction became Exo III-powered walking, i.e., the first stage of the cascade amplification system. After target DNA

hybridized with hpDNA, Exo III started to digest the DNA, initiated the walking process and released FAM into the supernatant. The supernatant was then collected for fluorescence detection. By using the fluorescent intensity of FAM in the supernatant for quantification, a detection limit of 30 fM for p53 was obtained (Figure 4B). Therefore, the signal amplification fold is 280/30 = 9.3 for walking stage.

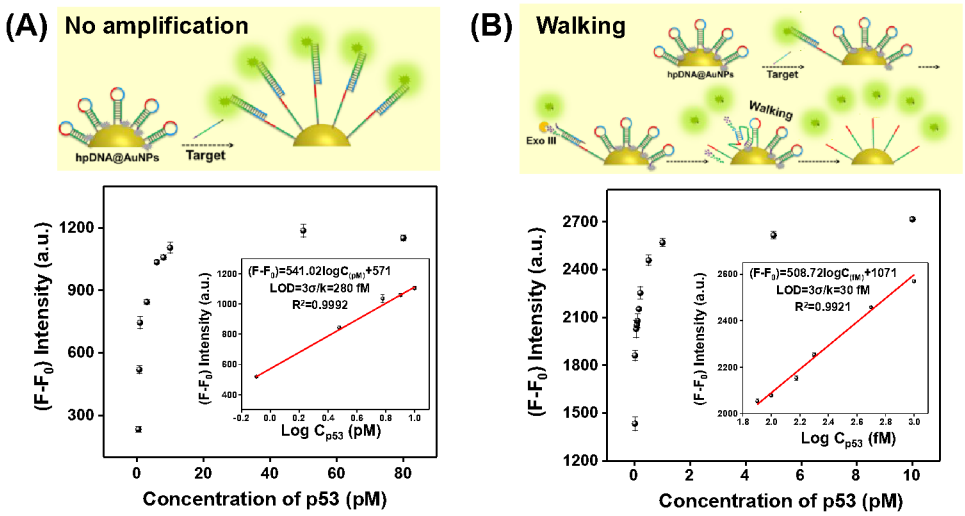


Figure 4. Schematic illustration and the calibration curve of the fluorescent detection system without amplification (A) and that with the walking amplification process (B).

By adding AgNCs@MNPs into the walking system, both rolling and walking proceeded. The fluorescent intensity of released AgNCs was used for quantification and the detection limit was calculated to be 13 fM (Figure S6), which means rolling has additional signal amplification of 30/13=2.3 folds on the basic of walking. However, the signal amplification efficiency of rolling is underestimated because of two reasons: (1) the fluorescence of AgNCs in the supernatant is seriously quenched by the co-existing AuNPs (Figure S7); (2) the fluorescence of AgNCs is not as strong as that of FAM. Therefore, the signal amplification efficiency of rolling should be much higher than just 2.3-fold improvement.

**Target DNA detection.** ICP-MS is very sensitive for metal ion quantifications, and one AgNC particle contains 10~100 of silver atoms. By digesting AgNCs into $Ag^+$ solutions by acids, one AgNC particle changes into tens to hundreds of silver ions. Therefore, by measuring the mass spectrometric signal of $^{107}Ag$, much lower detection limit can be obtained than that by measuring the fluorescence of AgNCs.

The detection limit is calculated to be 284 amol $L^{-1}$ by measuring the $^{107}Ag$ isotope by ICP-MS, which is ~45-fold lower than that using the fluorescence of AgNCs as signal output. Considering that the amount of AuNPs in the final supernatant is constant and Au can also be readily measured by ICP-MS, $^{197}Au$ isotope was employed as internal standard to perform ratiometric detection. As shown in Figure 5A-B, the $C_{Ag}/C_{Au}$ ratio increases gradually with the increase of p53 concentration, and a linear calibration graph, i.e., $C_{Ag}/C_{Au}$=1.056 logC + 1.08 ($R^2$=0.9918), is obtained versus the logarithm of p53 concentration within a range of 0.5-500 fmol $L^{-1}$. The limit of detection (LOD) was derived to be 119 amol $L^{-1}$, which is lower than that derived from $^{107}Ag$ isotope measurement (3SD/ slope, SD is the standard deviation of 10 blank samples[23-25]). The improvement on sensitivity of ratiometric detection may due to the reduction of blank signal fluctuation. The performance of the biosensor has a superior analysis capability compared with that of some previous reports based on other amplification strategies (Table 1).

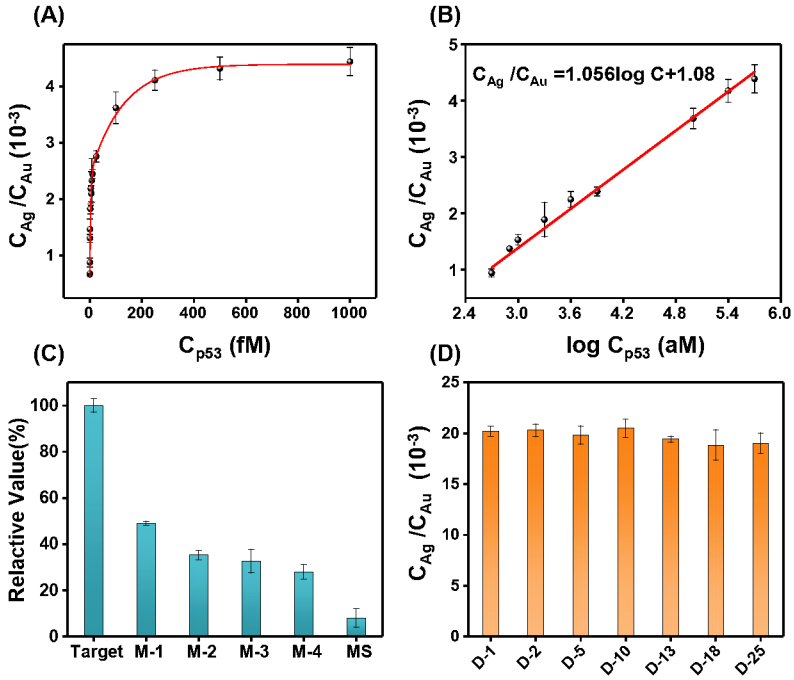


Figure 5. Analytical performance of the proposed ratiometric biosensor based on the ratio of

$C_{Ag}/C_{Au}$ under the optimized experiment conditions. (A) Variation of $C_{Ag}/C_{Au}$ intensity as a function of p53 concentration. (B) The linear relationship of the $C_{Ag}/C_{Au}$ intensity vs the logarithm of p53 concentration from 0.5 to 500 fM. (C) Selectivity of the proposed biosensor to the target, the single-base mismatch (M-1), two-base mismatch (M-2), three-base mismatch (M-3), four-base mismatch (M-4) and random sequences (MS). (D) ICP-MS signal of a sample with 1 pM target DNA in 25 days.

Table1. Comparison of this sensing system with reported methods for the assay of nucleic acid.

| **Target** | **Amplification strategy** | **Detection** | **LOD** | **Linear Range** | **Ref.** |
|---|---|---|---|---|---|
| miRNA | DNA walker | Electrochemical | 1.51 fM | 5.0 -5×$10^5$ fM | 24 |
| DNA | HCR | ECL | 15 fM | 25-1×$10^5$ fM | 25 |
| DNA | DNA walker | Fluorescence | 3.4×$10^3$ fM | (15 -370) ×$10^3$ fM | 26 |
| DNA | DNA walker | Electrochemical | 36 fM | 50 -500 fM | 27 |
| DNA | HCR | ICP-MS | 300 fM | 1×$10^3$ -1×$10^6$ fM | 28 |
| miRNA | HCR | ICP-MS | 0.041 fM | 0.1-500 fM | 29 |
| DNA | RCA+DNA walker | Fluorescence | 1.46 fM | 5-1.67 ×$10^3$ fM | 30 |
| DNA | CHA | Fluorescence | 4.7×$10^3$ fM | 0 -1.6 ×$10^7$ fM | 31 |
| DNA | DNA walker and rolling machine | ICP-MS | 0.119 fM | 0.5-500 fM | This work |

**Analytical performance and practical Applications.** The normal functioning of p53 is a potent barrier to cancer.[32] Cancer-associated mutations in p53 are a hallmark of most human cancers and cause dramatic defects in p53 function.[33] As the initiation of the DNA machine system requires precise base-pairing, the mismatch would lead to a low signal output. Therefore, our biosensor can be potentially used for the mutation point detection of target DNA. In the present study, a single-base-mutation DNA (M-1) closely related to cancers and other three imaginary mutant target DNAs with two, three, four mutation points and random sequence (MS) were interrogated under identical conditions to accurately assess the target recognition specificity. The analysis results are shown in Figure 5C. With ICP-MS response of the fully complementary target DNA (T) defined as 100%, the signals corresponding to

M-1, M-2, M-3, M-4 and MS are 49%, 35%, 32%, 28% and 8% respectively. It indicates that the biosensor is able to discriminate a one-nucleotide difference with high specificity. As shown in Figure 5D, ICP-MS signals are relatively stable during storage at 4°C for consecutive 25 days, which well demonstrates the long-term stability of the biosensor.

To explore the potential applications of this biosensing system in complex real biological sample matrixes, the spiking recovery experiments were conducted by detecting p53 in 10-fold diluted human serum samples from healthy volunteers. As shown in Table S3, p53 recovery within a range of 98%-106% is achieved, along with RSD of 2.8%-7.1%. This observation clearly illustrated that the designed biosensor provides promising potentials in the assay of complex biological samples.

## CONCLUSIONS

In summary, a smart DNA nanomachine was constructed for the sensitive and label-free detection of cancer-related DNA based on Exo III assisted cascade amplification strategy. The target DNA walks along the surface of hpDNA@AuNPs and trims the hpDNA with the assistance of Exo III for AuNPs to roll on MNPs surface. By changing the motion from stepwise walking to high-speed rolling, the derailment of walking leg is largely reduced and the processivity is further elevated, resulting in much improved signal amplification efficiency. Compared with 2D DNA rolling machine, the present strategy by integrating DNA walker and rolling cascade amplification allows roller to roll on a 3D DNA track, promoting the sensitivity to a new level. Furthermore, by employing the isotope signal of AuNPs as internal standard, a ratiometric detection by ICP-MS may be achieved, with more accurate and stable signal output with respect to those sensors with sole response readout.

## ASSOCIATED CONTENT

***Supporting Information**

The Supporting Information is available free of charge on the ACS Publications website at DOI: XXXX/XXX.

Materials and instrumentations used in this work; oligonucleotides sequences of DNA used in this work; operating conditions of ICP-MS instrument; UV-vis spectra of AuNPs and hpDNA@AuNPs; SEM, TEM and confocal fluorescent microscope images of MNPs and AgNCS@MNPs; The effect of dosage of AS strands, DNA@AgNCs and Exo III, as well as the effect of reaction time, temperature and pH on the performance of the biosensor; fluorescence spectra and calibration curve of the cascade amplification detection of 3D DNA walker and 3D DNA rolling machines with different concentrations of p53; the quenching effect of Toehold@AuNPs on DNA@AgNCs as a function of time; analysis results of p53 in human blood with detection by ICP-MS.

## AUTHOR INFORMATION

***Corresponding author.**

E-mail address: yangting@mail.neu.edu.cn (T. Yang).

Tel: +86 24 83688944; Fax: +86 24 83676698

†Na Wu and Kun Wang have equal contributions to this work.

**Conflicts of interest**

The authors declare no competing financial interest.

## ACKNOWLEDGEMENTS

Financial support from the Natural Science Foundation of China (21874014, 21727811, 21675019), the Fundamental Research Funds for the Central Universities (N180505021, N2005017, N2005027) are highly appreciated.

## ETHICAL STATEMENT

All experiments involving human serum samples are performed in compliance with the relevant laws and institutional guidelines and have been approved by the ethical committee of Northeastern University, China.

## REFERENCES

(1) Mason, S. D.; Tang, Y.; Li, Y.; Xie, X.; Li, F. Emerging Bioanalytical Applications of DNA Walkers. *TrAC Trends Anal Chem*. **2018**, 107, 212-221.

(2) Chen, J.; Lou, Z.; Sun, C.; Huang, Z.; Zhou, C.; Yin, S.; Duan, Y.; Li, Y. Research Progress of DNA walker and Its Recent Applications in Biosensor. *TrAC Trends Anal Chem*. **2019**, 120, 115626.

(3) Yan, T, T.; Zhu, L, Y.; Ju, H, X.; Lei, J, P. DNA-Walker-Induced Allosteric Switch for Tandem Signal Amplification with Palladium Nanoparticles/Metal-Organic Framework Tags in Electrochemical Biosensing. *Anal. Chem*. **2018**, 90, 14493-14499.

(4) Chen, J, B.; Zuehlke, A.; Deng, B.; Peng, H, Y.; Hou, X, D.; Zhang, H, Q. a Target-Triggered DNAzyme Motor Enabling Homogeneous Amplified Detection of Proteins. *Anal. Chem.* **2017**, 89, 12888-12895.

(5) Li, W.; Wang, L.; Jiang, W. A Catalytic Assembled Enzyme-Free Three-Dimensional DNA Walker and Its Sensing Application. *Chem. Commun*. **2017**, 53, 5527-5530.

(6) Peng, H. Y.; Li, X. F.; Zhang, H. Q.; Le, X. C. A MicroRNA-Initiated DNAzyme Motor Operating in Living Cells. *Nat. Commun*. **2017**, 8, 14378.

(7) Yuan, C. J.; Fang, J.; Duan, Q. Y.; Yan, Q.; Guo, J.; Yuan, T. X.; Gang, Y. Two-Layer Three-Dimensional DNA Walker with Highly Integrated Entropydriven and Enzyme-Powered Reactions for HIV Detection. *Biosens. Bioelectron*. **2019**, 133, 243-249.

(8) Yang, X. L.; Tang, Y. N.; Mason. D.; Li, F. Enzyme-Powered Three-Dimensional DNA Nanomachine for DNA Walking, Payload Release, and Biosensing. *ACS Nano*. **2016**, 10, 2324-2330.

(9) Li, Y. Y.; Wang, G. A.; Mason, S. D.; Yang, X. L.; Yu, Z. C.; Tang, Y. N.; Li, F. Simulation-Guided Engineering of an Enzyme Powered Three Dimensional DNA Nanomachine for Discriminating Single Nucleotide Variants. *Chem. Sci.* **2018**, 9, 6434-6439.

(10) Jiang, X. Y.; Wang, H. J.; Zhou, Y.; Yuan, R.; Chai, Y. Q. Electrochemiluminescence Biosensor Based on 3-D DNA Nanomachine Signal Probe Powered by Protein-Aptamer Binding Complex for Ultrasensitive Mucin 1 Detection. *Anal. Chem*. **2017**, 89, 4280-4286.

(11) Yang, T. Y.; Fang, J.; Guo, Y. C.; Sheng, S. C.; Pu, Q. L.; Zhang, L; Dai, L.; Xie, G, M. Fluorometric Determination of MicroRNA by Using an Entropy-Driven Three-Dimensional DNA Walking Machine Based on a Catalytic Hairpin Assembly Reaction on Polystyrene Microspheres. *Microchim. Acta*. **2019**, 186, 574.

(12) Li, D. D.; Xu, Y. X.; Fan, L.; Shen, B.; Ding, X. J.; Yuan, R.; Li, X. M. Target-Driven Rolling Walker Based Electrochemical Biosensor for Ultrasensitive Detection of Circulating Tumor DNA Using Doxorubicin@Tetrahedron-Au tags. *Biosens. Bioelectron*. **2020**, 148, 111826.

(13) Xu, Z. Q.; Chang, Y. Y.; Chai, Y. Q.; Wang, H. J.; Yuan, R. Ultrasensitive Electrochemiluminescence Biosensor for Speedy Detection of microRNA Based on a DNA Rolling Machine and Target Recycling. *Anal. Chem*. **2019**, 91, 4883-4888.

(14) Li, J. M.; Alexander, J.-B.; Yang, Y. R.; Shih, W. M.; Yan, H.; Walter, N. G.

Exploring the Speed Limit of Toehold Exchange with a Cartwheeling DNA Acrobat. *Nature. Nanotech.* **2018**, 13, 723-729.

(15) Wang, R.; Wang, L.; Xu, X. W. An Enzyme-Free and Label-Free Fluorescence Biosensor for MicroRNA Detection Based on Cascade Amplification of DNAzyme-Powered Three-Dimensional DNA Walker and Hybridization Chain Reaction. *Sens. Actuators.* B. **2018**, 268, 287-292.

(16) He, M. Q.; Wang, K.; Wang, W. J.; Yu, Y. L.; Wang, J. H. Smart DNA Machine for Carcinoembryonic Antigen Detection by Exonuclease III-Assisted Target Recycling and DNA Walker Cascade Amplification. *Anal Chem*. **2017**, 89, 9292-9298.

(17) Wu, T. T.; Cao, Y.; Yang, Y. M.; Zhang, X. Y.; Wang, S. T.; Xu, L. P.; Zhang, X. J. A Three-Dimensional DNA Walking Machine for the Ultrasensitive Dual-Modal Detection of MiRNA Using a Fluorometer and Personal Glucose Meter. *Nanoscale*. **2019**, 11, 11279-11284.

(18) Qu, X. M.; Zhu, D.; Yao, G. B.; Su, S.; Chao, J.; Liu, H.; Zou, X. L.; Wang, L. H.; Shi, J. Y.; Wang, L. H.; Huang, W.; Pei, H.; Fan, C. H. An Exonuclease III-Powered, On-Particle Stochastic DNA Walker. *Angew. Chem. Int. Ed.* **2017**, 56, 1855-1858.

(19) Kevin, Y.; Andrew, M.; Skanda, V.; Liu, Y.; Zhang, Y.; Fan, M. Z.; Eric, R. W.; Khalid, S. High-Speed DNA-Based Rolling Motors Powered by RNase H. *Nature. Nanotech*. **2015**, 11, 184-190.

(20) Cui, H. F.; Xu, T. B.; Sun, Y. L.; Zhou, A. W.; Cui, Y. H.; Liu, W.; Luong, H. T. John. Hairpin DNA as a Biobarcode Modified on Gold Nanoparticles for Electrochemical DNA Detection. ***Anal Chem.*** 2015, 87, 1358-1365.

(21) Zhou, W. J.; Zhu, J. B.; Fan, D. Q.; Teng, Y.; Zhu, X. Q.; Dong, S. J. A

Multicolor Chameleon DNA-Templated Silver Nanocluster and Its Application for Ratiometric Fluorescence Target Detection with Exponential Signal Response. *Adv. Funct. Mater.* **2017**, 27, 46, 1704092.

(22) Sarah, J. H.; Abigail, K. R.; Lytton, J.; Chad, A. M.; Maximizing DNA Loading on a Range of Gold Nanoparticle Sizes. *Anal. Chem.* **2006**, 78, 8313-8318.

(23). Zhou, H.; Duan, S, Y.; Huang, J.; He, F, J.; An Ultrasensitive Electrochemical Biosensor for Pseudomonas Aeruginosa Assay Based on a Rolling Circle Amplification-Assisted Multipedal DNA Walker. *Chem Comm*. **2020**, 56, 6273-6276.

(24) Peng, L, C.; Zhang, P.; Chai, Y, Q.; Yuan, R.; A Novel Bi-Directional DNA Walking Machine and Its Application in Enzyme-Free Electrochemiluminescence Biosensor for Sensitive Detection of MicroRNAs. *Anal. Chem*. **2017**, 89, 5036-5042.

(25) Chen, Y.; Xu, J.; Su, J.; Xiang, Y.; Yuan, R.; Chai, Y. Q. In Situ Hybridization Chain Reaction Amplification for Universal and Highly Sensitive Electrochemiluminescent Detection of DNA. *Anal Chem*. **2012**, 84, 7750-7755.

(26) Zhang, J.; Li, N. X.; Li, C. R.; Wang, X. X.; Liu, Y. C.; Mao, G. B.; Ji, X. H.; He, Z. K. A Nonenzymatic DNA Nanomachine for Biomolecular Detection by Target Rrecycling of Hairpin DNA Cascade Amplification. *Biosens Bioelectron*. **2018**, 107, 40-46.

(27) Wang, K.; He, M. Q.; Zhai, F. H.; Wang, J.; He, R. H.; Yu, Y. L. Autonomous DNA Nanomachine Based on Cascade Amplification of Strand Displacement and DNA Walker for Detection of Multiple DNAs. *Biosens Bioelectron*. **2018**, 105, 159-165.

(28) Deng, C.; Zhang, C. H.; Tang, H.; Jiang, J. H. ICP-MS DNA Assay Based on

Lanthanide Labels and Hybridization Chain Reaction Amplification. *Anal. Methods* **2015**, 7, 5767-5771.

(29) Liu, X.; Zhang, S. Q.; Ting, Y.; Yu, Y. L.; Wang, J. H. Highly Sensitive Detection of MicroRNA-21 with ICPMS via Hybridization Accumulation of Upconversion Nanoparticles. *Anal Chem*. **2018**, 90, 12116-12122.

(30) Zheng, J.; Ji, X. H.; Du, M. Y.; Tian, S. B.; He, Z. K. Rational Construction of A DNA Nanomachine for HIV Nucleic Acid Ultrasensitive Sensing. *Nanoscale* **2018**, 10, 17206-17211.

(31) Zhen, S, J.; Xiao, X.; Li, C. H.; Huang, C. Z. An Enzyme-Free DNA Circuit-Assisted Graphene Oxide Enhanced Fluorescence Anisotropy Assay for MicroRNA Detection with Improved Sensitivity and Selectivity. *Anal Chem*. **2017**, 89, 8766-8771.

(32) Miyashita, T.; Reed, J. C. Tumor Suppressor p53 Is a Direct Transcriptional Activator of the Human Bax Gene. *Cell.* **1995**, 80, 293-299.

(33) Levine, A. J.; Momand, J.; Finlay, C. A.; The p53 Tumour Suppressor Gene. *Nature.* **1991**, 351, 453-456

# For Table of Contents Only